Scintigraphic Evaluation of Experimental Chronic Osteomyelitis

Els Th.M. Dams, Marc W. Nijhof, Otto C. Boerman, Peter Laverman, Gert Storm, Pieter Buma,
J. Albert M. Lemmens, Jos W.M. van der Meer, Frans H.M. Corstens, and Wim J.G. Oyen

*Departments of Nuclear Medicine, Internal Medicine, Orthopedics, and Radiology, University Hospital Nijmegen,
Nijmegen; Department of Orthopedics, University Medical Center Utrecht, Utrecht; and Institute for Pharmaceutical Science,
Utrecht University, Utrecht, The Netherlands*

Assessment of disease activity and disease extent in chronic osteomyelitis remains a difficult diagnostic problem. Radiography is not particularly sensitive. Scintigraphic techniques can be more helpful, but the routinely available agents lack specificity (^{99m}Tc-methylene diphosphonate [MDP], ^{67}Ga-citrate) or are laborious to prepare (^{111}In-leukocytes). We evaluated the performance of 2 new radiopharmaceuticals, ^{99m}Tc-polyethyleneglycol (PEG) liposomes and ^{99m}Tc-hydrazinonicotinamide (HYNIC)-immunoglobulin G (IgG), in an experimental model of chronic osteomyelitis. **Methods:** Chronic osteomyelitis was induced in rabbits by inserting *S. aureus* into the right reamed and washed femoral canal. The canal was closed with cement. A sham operation was performed on the left femur. Routine radiographs were obtained immediately after surgery and before scintigraphy. Four weeks after surgery, each rabbit was injected with 37 MBq ^{99m}Tc-PEG liposomes, ^{99m}Tc-HYNIC-IgG, and ^{99m}Tc-MDP on 3 consecutive days and imaged up to 4 (MDP) or 22 (liposomes and IgG) h after injection. On day 4, rabbits received either 18 MBq ^{111}In-granulocytes or ^{67}Ga-citrate and were imaged up to 44 h after injection. Uptake in the infected femur was determined by drawing regions of interest. Ratios of infected-to-sham-operated femur were calculated. After the last image, the rabbits were killed, and the left and right femur were scored for microbiologic and histopathologic evidence of osteomyelitis. **Results:** ^{99m}Tc-PEG liposomes and ^{99m}Tc-HYNIC-IgG correctly identified all 6 rabbits with osteomyelitis. ^{111}In-granulocytes and ^{67}Ga-citrate gave equivocal results in 1 infected rabbit. ^{99m}Tc-MDP missed 1 case of osteomyelitis. The uptake in the affected region did not differ significantly between the agents, although ^{99m}Tc-MDP tended to have higher values (MDP, 4.75 $\pm$ 1.23 percentage injected dose per gram [%ID/g]; ^{67}Ga, 2.05 $\pm$ 0.54 %ID/g; granulocytes, 1.56 $\pm$ 0.83 %ID/g; liposomes, 1.75 $\pm$ 0.76 %ID/g, and IgG, 1.96 $\pm$ 0.27 %ID/g). The ratios of infected-to-normal femur were also not significantly different for the respective radiopharmaceuticals. Radiography visualized only severe osteomyelitis. **Conclusion:** In this rabbit model, ^{99m}Tc-PEG liposomes and ^{99m}Tc-HYNIC-IgG performed at least as well as ^{111}In-granulocytes and ^{67}Ga-citrate in the localization of chronic osteomyelitis. The ease of preparation, the better image quality, and the lower radiation dose suggest that ^{99m}Tc-PEG liposomes and ^{99m}Tc-HYNIC-IgG might be suitable alternatives for ^{67}Ga-citrate and ^{111}In-granulocytes in the scintigraphic evaluation of osteomyelitis.

Key Words: osteomyelitis; liposomes; immunoglobulin; granulocytes; white blood cells; ^{67}Ga; ^{99m}Tc; ^{111}In; bone scintigraphy; imaging

Chronic osteomyelitis is a disabling disease with a substantial impact on the quality of life (*1*). Accurate assessment of the severity and extent of the disease is essential to facilitate and optimize surgical or antibiotic treatment. For this purpose, different diagnostic modalities are available, including conventional radiography, CT, MRI, and scintigraphic techniques. Three-phase bone scanning with ^{99m}Tc-methylene diphosphonate (MDP) is an excellent tool for the initial evaluation of bone infection because of its high sensitivity (*2*). Its specificity, however, is rather low, because the agent accumulates in any area of increased bone turnover. This is a problem particularly when an additional pathologic condition is present, e.g., a fracture or an orthopedic device. In addition, the bone scan may be unsuitable for evaluation of installed therapy, as the findings may remain positive for months after clinical healing has occurred (*3*). Sequential ^{99m}Tc-MDP and ^{67}Ga-citrate scintigraphy have been reported to improve specificity in the diagnosis of chronic osteomyelitis (*4,5*). Unfortunately, ^{67}Ga-citrate also accumulates at sites of increased bone turnover, hampering correct interpretation in patients with violated bone. The role of ^{111}In-leukocytes in the diagnosis of chronic osteomyelitis remains controversial. Although some authors found only minimal uptake of labeled leukocytes in chronic, low-grade infection (*6*), others consider the technique to be the method of choice when bone scanning is equivocal (*2,7*). Major disadvantages of radiolabeled leukocytes are the laborious procedure required and the need to handle potentially contaminated blood.

New radiopharmaceuticals proposed for imaging of infection are radiolabeled nonspecific human immunoglobulin and radiolabeled liposomes. ^{111}In-immunoglobulin G (IgG) has been extensively studied in patients with musculoskel-

etal infections, and the agent has shown high accuracy in chronic osteomyelitis (8). We recently showed that IgG labeled to ^{99m}Tc using hydrazinonicotinamide (^{99m}Tc-HYNIC-IgG) performed equally as well as ^{111}In-IgG in patients with nonacute infection, including some patients with chronic osteomyelitis (9). The application of radiolabeled liposomes for imaging purposes has regained interest with the development of liposomes with long-circulating characteristics (10,11). These so-called sterically stabilized liposomes, coated with polyethyleneglycol (PEG) and radiolabeled with ^{111}In or ^{99m}Tc, showed favorable performance compared with routine agents in various experimental models of acute infection (12,13). A new ^{99m}Tc labeling method, using HYNIC as a chelator, was recently introduced and showed improved in vitro and in vivo characteristics of radiolabeled PEG liposomes compared with the conventional ^{99m}Tc-hexamethyl propyleneamine oxime labeling method (14). However, the performance of radiolabeled liposomes has not been evaluated in a model of chronic infection. Because a ^{99m}Tc label is preferred over ^{111}In, on account of better imaging properties and lower radiation dose, we evaluated ^{99m}Tc-HYNIC-PEG liposomes and ^{99m}Tc-HYNIC-IgG in a rabbit model of chronic osteomyelitis. For comparison, we included the conventional and well-established agents ^{99m}Tc-MDP, ^{67}Ga-citrate, and ^{111}In-granulocytes.

MATERIALS AND METHODS

Animal Model

Animals. Adult female New Zealand White rabbits ranging in weight from 2.8 to 3.2 kg were caged individually and fed with regular rabbit diet and water ad libitum.

Osteomyelitis Model. The experiments described in this article were performed in accordance with the guidelines of the local animal welfare committee. Chronic osteomyelitis was induced in 9 rabbits as described previously, with minor modifications (15,16). Briefly, the rabbits were anesthetized with a mixture of halothane, nitrous oxide, and oxygen, and placed prone on the operation table. Both hind legs were shaved, disinfected with a 2% tincture of iodine, and isolated by sterile drapes. The trochanter tertius was exposed bilaterally, and the cortex was penetrated using an air-pressured AO minidrill (Synthes, Detlach, Switzerland). The hole was widened, and the femoral canal was reamed with drills and fraises. The medullary canal was washed with sterile saline solution and suctioned. A small syringe with a 2-mm-long silicone tube (outer diameter, 3.0 mm) attached was filled with bone cement (Howmedica Inc., Rutherford, NJ) and placed in an applicator gun, and approximately 1.2 mL cement was injected gently into the right femoral canal. The left femoral canal was then inoculated with 1 million colony-forming units *Staphylococcus aureus* (ATCC 25923; American Type Culture Collection, Manassas, VA) and closed with bone cement as described above. After polymerization of the cement, the wounds at both sides were cleaned with sterile saline solution and closed. Clinical examination was performed regularly with special attention to wound healing, activity level, body temperature, and body weight.

Radiopharmaceuticals

^{99m}Tc-PEG-HYNIC Liposomes. PEG-HYNIC liposomes were prepared as described previously (14). The liposomes were com-posed of the polyethyleneglycol-2000 derivative of distearoylphosphatidyl-ethanolamine (PEG-DSPE), partially hydrogenated egg-phosphatidylcholine, cholesterol, and the hydrazino-nicotinamide derivative of distearoylphosphatidyl-ethanolamine (HYNIC-DSPE) in a molar ratio of 0.15:1.85:1:0.07. The particle size distribution was determined by dynamic light scattering with a Malvern 2000 system equipped with a 25-mW neon laser (Malvern Instruments Ltd., Malvern, UK). As a measure of particle size distribution of the dispersion, the polydispersity index was determined. This index ranges from 0.0 for an entirely monodisperse dispersion to 1.0 for a completely polydisperse dispersion. The mean size of the liposome preparations was 85 nm, with a polydispersity index of 0.1. Preformed HYNIC-PEG liposomes were labeled with ^{99m}Tc as previously described (14). ^{99m}Tc-labeled HYNIC liposomes have been shown to be highly stable. No significant release of radiolabel was observed after incubation with high concentrations of diethylenetriamine pentaacetic acid, cysteine, or glutathione or after 48 h of incubation in serum at 37°C (14). The radiochemical purity of the PEG liposomes was determined using instant thin-layer chromatography (ITLC) on ITLC-SG strips (Gelman Sciences, Inc., Ann Arbor, MI) with 0.15 mol/L sodium citrate (pH, 5.0) as the mobile phase and verified by elution on a PD-10 column. Labeling efficiency exceeded 95%, and the ^{99m}Tc-liposomes were administered intravenously without any further purification (37 MBq per rabbit).

^{99m}Tc-HYNIC-IgG. HYNIC was synthesized and conjugated to human polyclonal IgG (Gammagard; Baxter/Hyland, Lessines, Belgium) according to the method described by Abrams et al. (17). The purified HYNIC-conjugated IgG was diluted to 4 mg/mL in 0.15 mol/L acetate (pH, 5.85), sterilized by membrane filtration, and stored at −20°C in 0.5-mL aliquots. After thawing of 0.5 mL of the HYNIC IgG conjugate, the conjugate was radiolabeled with ^{99m}Tc by adding 0.1 mg N-[Tris(hydroxymethyl)methyl]glycine (Fluka, Buchs, Switzerland), 0.01 mg SnSO$_4$, and 400 MBq ^{99m}Tc-pertechnetate. The mixture was incubated for 15 min at room temperature. The radiochemical purity of radiolabeled IgG was determined by ITLC on silica gel strips with 0.15 mol/L sodium acetate (pH, 5.85) as the mobile phase. High-performance liquid chromatography analysis of the ^{99m}Tc-HYNIC-IgG preparation on a size-exclusion column (Protein Pak 300 SW; Waters Associates, Milford, MA) revealed that the preparation migrated as a monomeric 150-kDa peak (<5% aggregates) as has been described (18). Labeling efficiency was always >95%. Each rabbit received a dose of 0.2 mg IgG labeled with approximately 37 MBq ^{99m}Tc.

^{67}Ga-Citrate. ^{67}Ga-citrate (DRN 3103) was purchased from Mallinckrodt, Inc. (Petten, The Netherlands). A dose of approximately 18 MBq ^{67}Ga-citrate per rabbit was injected intravenously.

^{111}In-Granulocytes. Carotid artery canulation was performed on 2 anesthetized donor rabbits. A total of 100 mL blood was drawn into acid citrate dextrose-coated tubes. The total leukocyte count of the donor rabbits was 6.4 and 6.8 × 10^9/L, respectively, with approximately 50% granulocytes. Separation of granulocytes was performed according to the method described by Lillevang et al. (19) with minor modifications (20). As we have shown previously, this separation procedure did not affect granulocyte function (20). Morphologic integrity of the granulocytes was checked by light microscopy. Granulocyte purity (Giemsa-stained slides) was >90%. Functional integrity of the labeled granulocytes was checked by trypan blue staining, indicating that cell viability exceeded 98%. In addition, granulocyte function was evaluated by in vivo performance, including transit through the lungs and recovery of labeled

granulocytes in the blood. The labeling efficiency was 86%. A dose of 18 MBq ^{111}In-granulocytes was administered intravenously.

^{99m}Tc-MDP. A kit containing methylenediphosphonate and stannous chloride was labeled with ^{99m}Tc, with a labeling efficiency of >95% as determined by ITLC. A dose of 18 MBq ^{99m}Tc-MDP was administered intravenously.

Study Design

All rabbits underwent studies with ^{99m}Tc-liposomes, ^{99m}Tc-IgG, and ^{99m}Tc-MDP to minimize bias caused by variation in the degree of infection. The relatively long half-lives of ^{111}In and ^{67}Ga precluded serial injection. Therefore, the animals were then randomized into 2 groups to receive either ^{67}Ga-citrate or ^{111}In-leukocytes. Scintigraphic studies were started 4 wk after surgery. The radiopharmaceuticals were injected in a fixed order. On day 1 of the imaging experiment, ^{99m}Tc liposomes were injected. ^{99m}Tc-IgG was administered on day 2, followed 1 d later by ^{99m}Tc-MDP. On day 4, 1 group of rabbits received ^{111}In-granulocytes and the other group received ^{67}Ga-citrate. The rabbits were slightly sedated by a subcutaneous injection of 0.2 mL Hypnorm (fentanyl, 0.315 mg/mL, and fluanisone, 10 mg/mL; Janssen Pharmaceutical, Oxford, UK). After sedation, the rabbits were immobilized in a mold and placed prone on a γ camera equipped with a parallel-hole, low-energy collimator (Orbiter; Siemens Medical Systems Inc., Hoffman Estates, IL) for the ^{99m}Tc studies and a medium-energy collimator for the ^{67}Ga and ^{111}In studies. Imaging was performed at 5 min and 1, 4, 10, 22, and 44 h after injection of ^{111}In or ^{67}Ga. Imaging with ^{99m}Tc-MDP was performed at 3 min after injection (blood-pool image) and at 1 and 4 h after injection (delayed images). Images (250,000 counts/image, except the 22-h postinjection image [100,000 counts/image]) were obtained and stored in a 256 × 256 matrix.

The scintigraphic results were analyzed quantitatively and qualitatively. Regions of interest (ROI) were drawn over the infected right femur and sham-operated left femur and over the whole body. Additional ROIs over the lungs were drawn on the scintigrams of rabbits injected with ^{111}In-labeled granulocytes. Ratios of infected right femur to sham-operated left femur were calculated. Residual activity at the osteomyelitis site compared with whole-body activity was also calculated. Counts were corrected for differences in the numbers of pixels before calculating ratios and percentages. All scans were also evaluated qualitatively without knowledge of the histopathologic outcome. Scan findings were considered positive if focal accumulation of radioactivity at the osteomyelitis site exceeded the uptake at the sham-operated site or if inhomogeneously enhanced accumulation was present at the osteomyelitis site.

A separate group of 2 noninfected rabbits was injected with ^{111}In-granulocytes to calculate granulocyte recovery. Serial blood samples were taken at 5, 15, 30, and 45 min and 1, 2, 4, and 22 h after injection.

Assessment

The results of the scintigraphic studies were compared with the results of radiologic, microbiologic, and histopathologic examination. Conventional radiographs were obtained immediately after surgery and before additional imaging was performed. Unaware of the results of all other procedures, observers evaluated the radiograms with respect to 3 parameters: periostal reaction, new bone formation, and extent of bone destruction (21). Immediately after completion of the scintigraphic studies, the rabbits were killed with an overdose of sodium phenobarbital. The left and right femurs

from all animals were excised and cleaned of tissue debris. The distal ends were removed and the femur was cut longitudinally in 2 halves, using a high-speed dental drill with a circular metal saw. The bone cement was carefully removed. The external surface of the bone specimen was thoroughly cleaned with alcohol. One bone specimen of each femur was sent for microbiologic examination. The other bone specimens were fixed in 4% buffered formalin and decalcified in 10% ethylenediamine tetraacetic acid. Longitudinal sections were made, slide mounted, and stained with hematoxylin and eosin. All sections were reviewed with light microscopy with respect to 4 parameters: necrotic bone, purulent inflammation, periostal new bone, and granulation tissue. The presence of osteomyelitis was confirmed on the basis of these histopathologic findings.

Statistical Analysis

All mean values are given as percentage injected dose per gram (%ID/g) or ratios ± 1 SEM. One-way ANOVA was used to compare the uptake at the osteomyelitis site and the sham-surgery site for the different agents. In addition, the repeated-measures ANOVA model was used to evaluate differences among the imaging times for each agent. The level of significance was set at $P < 0.05$.

RESULTS

One of the 9 rabbits died of a *Klebsiella* species sepsis 2 d after surgery. A second rabbit died of unknown causes after ^{99m}Tc-HYNIC-PEG liposomes and ^{99m}Tc-HYNIC-IgG scintigraphy. In this rabbit, both studies were positive for infection, confirmed by histopathologic examination. The following section refers to the data of the 7 rabbits that completed all studies.

Postoperative radiographs showed no fractures or cement outside the femur. Of the 7 rabbits, 6 were found to have histopathologic evidence of chronic osteomyelitis in the right femur. In 4 of these rabbits, the infection was confined to the distal femur, whereas in 2 the infection extended toward the proximal femur. The right limb of the osteomyelitis-negative rabbit showed only minimal leukocytic infiltration, which was found to be consistent with a foreign body reaction. None of the sham-operated left limbs showed any sign of infection. The microbiologic studies of the bone specimens were concordant with histopathologic findings in 5 of the 6 infected rabbits and confirmed the presence of *Staphylococcus aureus* infection. In contrast, radiologic findings were abnormal in only 2 of these rabbits, showing periosteal elevation and new bone formation at the site of the infection. Scintigraphic analysis was performed on the images of all 7 rabbits. For comparison of the absolute and relative uptake of the respective agents at the osteomyelitis site, only the data of the 6 infected rabbits were used. A summary of the results is given in Table 1.

Examples of scintigraphic recordings of the 5 radiopharmaceuticals are shown in Figure 1. Scintigraphy with ^{99m}Tc-HYNIC-PEG liposomes and ^{99m}Tc-HYNIC-IgG visualized the infected femur in all 6 osteomyelitis-positive rabbits. In contrast, scintigraphy with both ^{67}Ga-citrate and ^{111}In-granulocytes gave equivocal results in 1 infected

TABLE 1
Results of Scintigraphic, Radiologic, Microbiologic, and Histopathologic Procedures in Rabbits with Chronic Osteomyelitis

Rabbit no.	MDP 4 h p.i.	22 h p.i.		44 h p.i.		Radiology	Histology	Culture
		Liposomes	IgG	111In-granulocytes	67Ga citrate			
1	+	+	+	+	NP	+	+	+
2	+	+	+	NP	+	+	+	+
3	+	+	+	NP	+	−	+	+
4	+	+	+	+	NP	−	+	+
5	+	+	+	NP	±	−	+	+
6	−	+	+	±	NP	−	+	−
7	±	+	+	±	NP	−	−	−

MDP = ^{99m}Tc-MDP; p.i. = after injection; liposomes = ^{99m}Tc-PEG liposomes; IgG = ^{99m}Tc-HYNIC-IgG; + = positive; NP = not performed; − = negative; ± = equivocal.

rabbit. Both rabbits had moderate infection confined to the distal femur. ^{99m}Tc-MDP findings were falsely negative in 1 of these rabbits. A false-positive result was noted with ^{99m}Tc-HYNIC-PEG liposomes and ^{99m}Tc-HYNIC-IgG in the osteomyelitis-negative rabbit. In this case, the scintigrams of ^{99m}Tc-MDP and ^{111}In-granulocytes were classified as equivocal (^{67}Ga-citrate was not performed). The cellular infiltration seen on histopathologic examination, albeit minimal, probably explained the false-positive result. In 5 of the 6 infected rabbits, scintigraphy with ^{99m}Tc-HYNIC-PEG liposomes and ^{99m}Tc-HYNIC-IgG gave positive results as soon as 4 h after injection. At 22 h after injection, however, visualization of the infection was improved as a result of increasing focal uptake and decreasing background activity. With ^{67}Ga-citrate and ^{111}In-granulocytes, the osteomyelitis could be identified first on the 22-h images. However, with both agents visualization of the infected femur was better on the 44-h images, as a result of improved background clearance.

Results of the quantitative analysis of the images are shown in Figure 2. Although ^{99m}Tc-MDP tended to have higher values for uptake in the infected femur, the differences with the other agents were statistically not significant. The residual activity at the osteomyelitis site as a fraction of the whole-body activity, however, was significantly higher than that of the other four agents, because of the rapid whole-body clearance of ^{9m}Tc-MDP ($P < 0.01$; data not shown). ^{99m}Tc-HYNIC-PEG liposomes, ^{99m}Tc-HYNIC-IgG, ^{67}Ga-citrate, and ^{111}In-granulocytes displayed very similar absolute uptake values at all time points ranging from 1.6 to 2.0 %ID/g in the final image (Fig. 2). As shown in Figure 3,
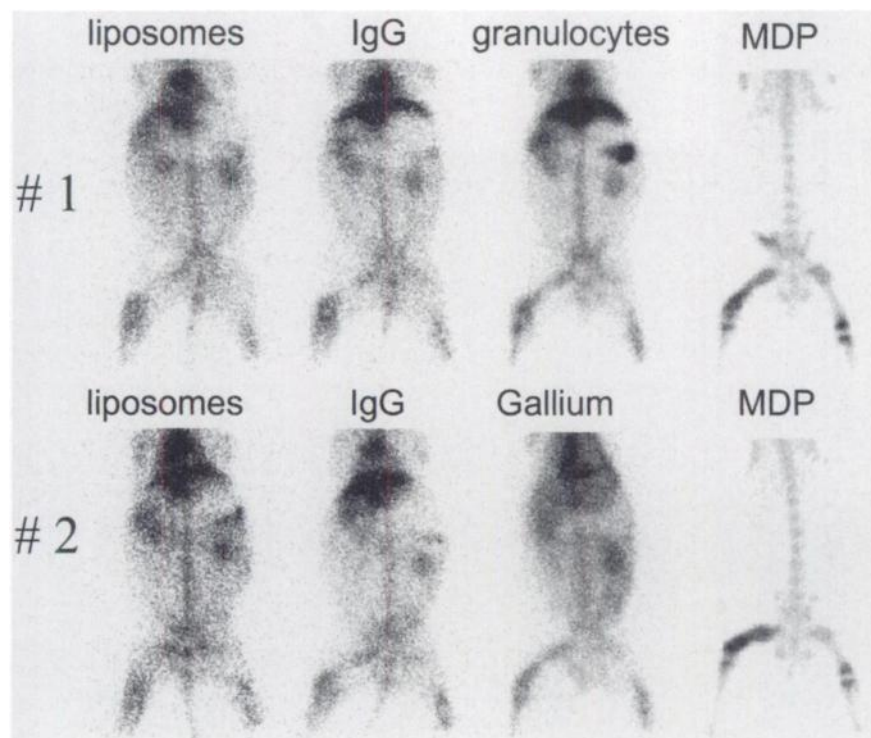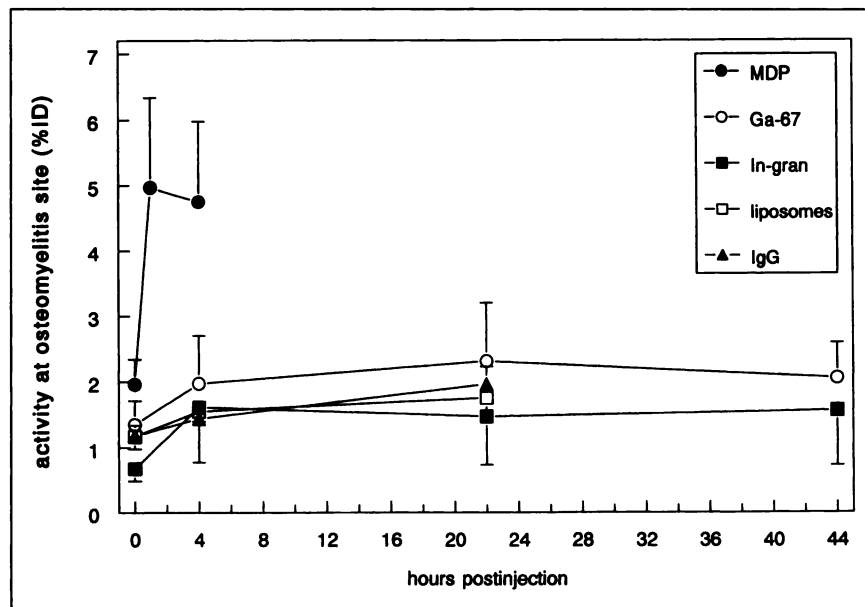

FIGURE 1. Scintigraphic images of 2 rabbits with chronic osteomyelitis after injection of ^{99m}Tc-MDP (4 h after injection), ^{99m}Tc-PEG liposomes (22 h after injection), ^{99m}Tc-HYNIC-IgG (22 h after injection), ^{111}In-granulocytes (44 h after injection, rabbit 1), and ^{67}Ga-citrate (44 h after injection, rabbit 2). Focal uptake of respective agents in infected femur is clearly visible.

FIGURE 2. Activity uptake at osteomyelitis site as determined by quantitative analysis of scintigraphic images of rabbits injected with ^{99m}Tc-MDP (●), ^{99m}Tc-PEG liposomes (□), ^{99m}Tc-HYNIC-IgG (▲), ^{111}In-granulocytes (■), and ^{67}Ga-citrate (○), comparing uptake at osteomyelitis site. Error bars represent SEM.

ratios of infected to sham-operated site were similar for all 5 radiopharmaceuticals. In accordance with the qualitative assessment of infection, the ratios for both ^{99m}Tc-HYNIC-PEG liposomes and ^{99m}Tc-HYNIC-IgG increased over time, up to 22 h after injection (1.31 ± 0.09 and 1.36 ± 0.13, respectively, at 4 h after injection and 1.44 ± 0.08 and 1.64 ± 0.14, respectively, at 22 h after injection; $P < 0.05$). The difference between the mean ratios of ^{67}Ga-citrate and ^{111}In-granulocytes in the 22- and 44-h images, as a function of time, was statistically not significant (1.46 ± 0.17 versus 1.50 ± 0.30, respectively, and 1.53 ± 0.14 versus 1.54 ± 0.30, respectively; $P > 0.05$), which also correlated with the qualitative analysis of the scintigrams.
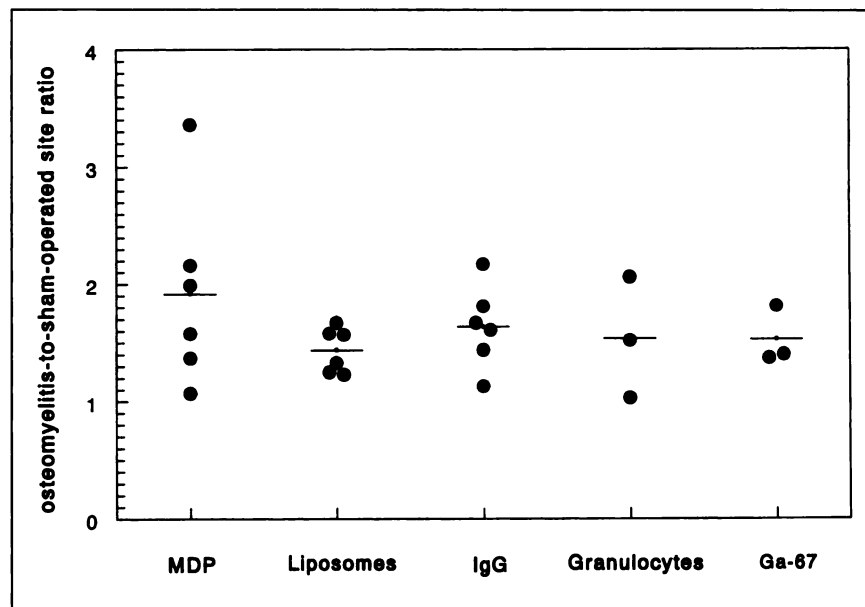
Quantitative analysis of the scintigrams of ^{111}In-granulocytes showed rapid initial lung transit, indicating that the labeling procedure had not affected granulocyte function (Fig. 4). In addition, granulocyte recovery at 45 min was >40% (Fig. 4), confirming preserved granulocyte integrity (22).

DISCUSSION

This study showed excellent performance by 2 new scintigraphic agents, ^{99m}Tc-IgG and ^{99m}Tc-PEG liposomes, to visualize osteomyelitis. These new agents performed at least as well as ^{67}Ga-citrate and ^{111}In-granulocytes in the localization of chronic bone infection. Both ^{99m}Tc-PEG liposomes and ^{99m}Tc-HYNIC-IgG have the major advantage of a ^{99m}Tc label, providing a high photon flux at early time points after injection in combination with a low radiation dose, low costs, and continuous availability. In addition,

FIGURE 3. Ratios of osteomyelitis to sham-operated site at 4 h (^{99m}Tc-MDP), 22 h (^{99m}Tc-PEG liposomes and ^{99m}Tc-HYNIC-IgG), and 44 h (^{111}In-granulocytes and ^{67}Ga-citrate) after injection, calculated from quantitative ROI analyses of scintigraphic images. Horizontal bars represent mean values.
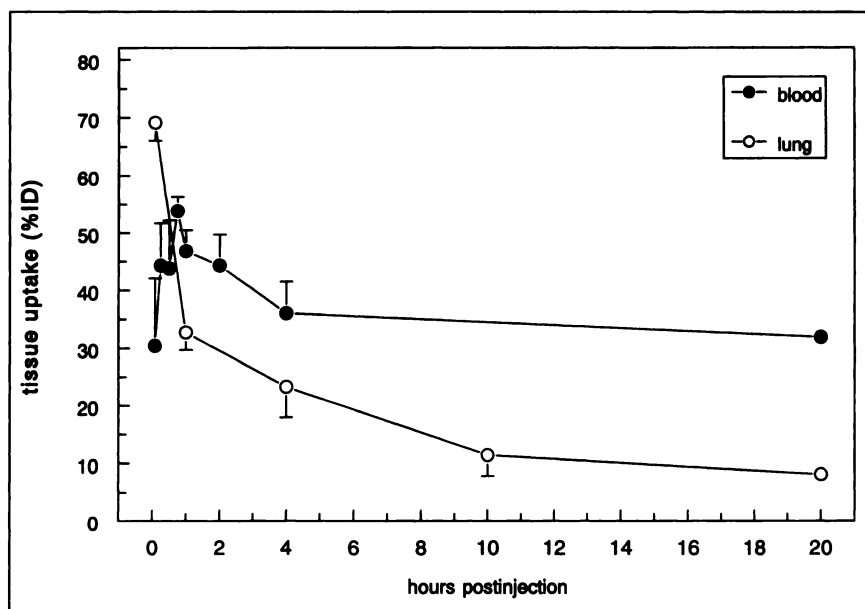
FIGURE 4. In vivo measurements of granulocyte function. Blood clearance of ^{111}In-leukocytes, calculated from serial blood samples (●). Lung clearance of ^{111}In-granulocytes, determined by quantitative analysis of scintigraphic images of rabbits injected with ^{111}In-granulocytes (O). Error bars represent SEM.

both agents are easy to prepare and do not require handling of potentially contaminated blood. The lack of false-negative results for both agents refutes concern that a ^{99m}Tc label would be less suited for the detection of low-grade osteomyelitis (23). Indeed, most infected rabbits were identified as early as 4 h after injection. With ^{99m}Tc-PEG liposomes as well as with ^{99m}Tc-HYNIC-IgG, all infectious sites were detected, whereas ^{67}Ga-citrate and ^{111}In-leukocytes each missed 1 case of osteomyelitis.

Awasthi et al. (24) showed that radiolabeled liposomes were very effective in the evaluation of acute osteomyelitis in rabbits (24). The target-to-nontarget ratios obtained with labeled liposomes in this study were slightly lower than those found in their study. This difference can be explained quite easily by the fact that in the latter study no sham procedure was performed. In addition, because focal accumulation of liposomes is thought to depend on increased vascular permeability (25), uptake of the agent is expected to be lower in chronic than in acute inflammation. The lower ratios apparently did not compromise accurate qualitative assessment, probably because the pattern of uptake of the radiolabel contributed to delineation of the infection.

[111]In-labeled IgG has been shown to be very suitable for the evaluation of patients with musculoskeletal infections, including chronic osteomyelitis (8). ^{99m}Tc-HYNIC-IgG has demonstrated efficacy equal to that of ^{111}In-IgG in this patient category (9). The results of our study confirm the ability of ^{99m}Tc-HYNIC-IgG to detect chronic, low-grade infection.

The high uptake of ^{99m}Tc-MDP at the osteomyelitis site did not result in improved infection-to-sham-surgery ratios compared with the other agents. In fact, the absolute uptake of the agent at the distal femur in the false-negative case was as high as 2 %ID/g. Therefore, despite high absolute uptake in the infected site, the ratio was only 1.07, illustrating the

increased uptake of the agent at sites of bone repair for any cause. In contrast, for ^{67}Ga-citrate both absolute uptake and infection-to-sham ratio were similar to the values obtained with the other non–bone-seeking agents, indicating that accumulation of ^{67}Ga-citrate at the sham-surgery site was relatively low. Despite the similar uptake and ratios, ^{67}Ga-citrate and ^{111}In-leukocyte scintigraphy appeared to have lower sensitivity for the detection of infection than did ^{99m}Tc-PEG-liposomes and ^{99m}Tc-HYNIC-IgG. This discrepancy probably resulted from the suboptimal imaging characteristics of both ^{67}Ga and [111]In.

The low yield of radiography in this study confirmed that this technique is unreliable in establishing bone infection when an additional pathologic condition is present (2).

The use of labeled granulocytes in a rabbit model of chronic inflammation has its pitfalls. Because rabbit leukocytes are easily damaged by handling (19), the separation procedure could have negatively biased their performance. In this study, we were able to establish preserved granulocyte function by means of in vivo tests, which are reliable markers of leukocyte damage (22). The predominance of mononuclear cells, such as lymphocytes and macrophages, in areas of chronic infection raises the question of whether the use of a granulocyte-enriched preparation in this model was justified. Indeed, some authors favor the use of a mixed-cell preparation in chronic inflammation (26,27). More recently, however, it has been shown that ^{111}In-labeled lymphocytes actively eliminated the radiolabel, arguing against the concept that lymphocytes contribute to a positive image in chronic inflammation (28,29). Using a granulocyte-enriched mixture, we maximized the activity made available to the infectious lesion, in accordance with the guidelines of Peters (28). Still, the equivocal result in 1 infected rabbit was a result of the relatively mild infection in that animal.

CONCLUSION

In this rabbit model of chronic osteomyelitis, ^{99m}Tc-PEG-liposomes and ^{99m}Tc-HYNIC-IgG performed at least as well as ^{111}In-granulocytes and ^{67}Ga-citrate. Although the latter 2 agents each gave 1 equivocal result, labeled liposomes and labeled IgG correctly identified all infectious lesions. The absolute uptake and target-to-nontarget ratios were very similar for the 4 agents. ^{99m}Tc-MDP gave 1 false-negative result because of high uptake at the sham-operated site, illustrating the nonspecific accumulation of this agent in areas of increased bone turnover. Because both ^{99m}Tc-PEG-liposomes and ^{99m}Tc-HYNIC-IgG display favorable dosimetric and physical characteristics and are easy to prepare, they can be valuable agents for the evaluation of chronic osteomyelitis.

ACKNOWLEDGMENTS

REFERENCES

1. Lew DP, Waldvogel FA. Osteomyelitis. *N Engl J Med.* 1997;336:999–1007.
2. Elgazzar AH, Abdel Dayem HM, Clark JD, Maxon HR. Multimodality imaging of osteomyelitis. *Eur J Nucl Med.* 1995;22:1043–1063.
3. Scoles PV, Hilty MD, Sfakianakis GN. Bone scan patterns in acute osteomyelitis. *Clin Orthop.* 1980;153:210–217.
4. Tumeh SS, Aliabadi P, Weissman BN, McNeil BJ. Chronic osteomyelitis: bone and gallium scan patterns associated with active disease. *Radiology.* 1986;158:685–688.
5. Palestro CJ. The current role of gallium imaging in infection. *Semin Nucl Med.* 1994;24:128–141.
6. Propst-Proctor SL, Dillingham MF, McDougall IR. The white blood cell scan in orthopedics. *Clin Orthop.* 1982;168:157–165.
7. Johnson JA, Christie MJ, Sandler MP, Parks PF Jr, Homra L, Kaye JJ. Detection of occult infection following total joint arthroplasty using sequential technetium-99m HDP bone scintigraphy and indium-111 WBC imaging. *J Nucl Med.* 1988;29:1347–1353.
8. Oyen WJG, van Horn JR, Claessens RAMJ, Slooff TJJH, van der Meer JWM, Corstens FHM. Diagnosis of bone, joint and joint prosthesis infections with In-111 labeled nonspecific human immunoglobulin G scintigraphy. *Radiology.* 1992;182:195–199.
9. Dams ET, Oyen WJ, Boerman OC, et al. Technetium-99m labeled to human immunoglobulin G through the nicotinyl hydrazine derivative: a clinical study. *J Nucl Med.* 1998;39:119–124.
10. Bakker-Woudenberg IA, Lokerse AF, ten Kate MT, Mouton JW, Woodle MC, Storm G. Liposomes with prolonged blood circulation and selective localization in *Klebsiella pneumoniae*-infected lung tissue. *J Infect Dis.* 1993;168:164–171.
11. Woodle MC, Lasic DD. Sterically stabilized liposomes. *Biochem Biophys Acta.* 1992;1113:171–199.
12. Oyen WJ, Boerman OC, Storm G, et al. Detecting infection and inflammation with technetium-99m-labeled Stealth liposomes. *J Nucl Med.* 1996;37:1392–1397.
13. Boerman OC, Storm G, Oyen WJ, et al. Sterically stabilized liposomes labeled with indium-111 to image focal infection. *J Nucl Med.* 1995;36:1639–1644.
14. Laverman P, Dams ETM, Oyen WJG, et al. A novel method to label liposomes with Tc-99m via the nicotinyl hydrazino derivative. *J Nucl Med.* 1999;40:192–197.
15. Nijhof MW, Dhert WJA, Vogely HC, Fleer A, Verbout AC. Prevention of *S. aureus* and *S. epidermidis* infection by tobramycin-containing bone cement. Paper presented at: Annual Meeting of the Orthopaedic Research Society; February 3, 1999; Anaheim, CA.
16. Nijhof MW, Dhert WJA, Tilman PBJ, Verbout AJ, Fleer A. Release of tobramycin from tobramycin-containing bone cement in bone and serum of rabbits. *J Mat Science.* 1997;8:799–802.
17. Abrams MJ, Juweid M, tenKate CI, et al. Technetium-99m-human polyclonal IgG radiolabeled via the hydrazino nicotinamide derivative for imaging focal sites of infection in rats. *J Nucl Med.* 1990;31:2022–2028.
18. Claessens RAMJ, Boerman OC, Koenders EB, Oyen WJG, van der Meer JWM, Corstens FHM. Technetium-99m labelled hydrazinonicotinamido human non-specific polyclonal immunoglobulin G for detection of infectious foci: a comparison with two other technetium-labelled immunoglobulin preparations. *Eur J Nucl Med.* 1996;23:414–421.
19. Lillevang ST, Toft P, Nilsen B. A method for isolating granulocytes from rabbit blood without causing activation. *J Immunol Methods.* 1994;169:137–138.
20. Dams ET, Oyen WJG, Boerman OC, et al. Tc-99m-labeled liposomes to image experimental colitis in rabbits: comparison with Tc-99m-HMPAO-granulocytes and Tc-99m-HYNIC-IgG. *J Nucl Med.* 1998;39:2172–2178.
21. Norden CW, Myerowitz RL, Keleti E. Experimental osteomyelitis due to *S. aureus* and *P. aeruginosa*: a radiographic pathological correlative analysis. *Br J Exp Pathol.* 1980;61:451–460.
22. Peters AM, Roddie ME, Danpure HJ, et al. ^{99}Tcm-HMPAO labelled leukocytes: comparison with ^{111}In-tropolonate labelled granulocytes. *Nucl Med Commun.* 1988;9:449–463.
23. Oyen WJG, Claessens RAMJ, van Horn JR, van der Meer JWM, Corstens FHM. Scintigraphic detection of bone and joint infections with indium-111 labeled nonspecific polyclonal human immunoglobulin G. *J Nucl Med.* 1990;31:403–412.
24. Awasthi V, Goins B, Klipper R, Loredo R, Korvick D, Phillips WT. Imaging experimental osteomyelitis using radiolabeled liposomes. *J Nucl Med.* 1998;39:1089–1094.
25. Morrel EM. Autoradiographic method for quantitation of radiolabeled proteins in tissues using indium-111. *J Nucl Med.* 1989;30:1538–1545.
26. Datz FL. Indium-111-labeled leukocytes for the detection of infection: current status. *Semin Nucl Med.* 1994;24:92–109.
27. Schauwecker DS, Burt RW, Park HM, et al. Comparison of purified indium-111 granulocytes and indium-111 mixed leukocytes for imaging of infections. *J Nucl Med.* 1988;29:23–25.
28. Peters AM. The choice of an appropriate agent for imaging inflammation. *Nucl Med Commun.* 1996;17:455–458.
29. Kuyama J, McCormack A, George AJ, et al. Indium-111 labelled lymphocytes: isotope distribution and cell division. *Eur J Nucl Med.* 1997;24:488–496.